

## Luminescent and structural properties of ZnO nanorods prepared under different conditions

V. A. L. Roy

*Department of Electrical and Electronic Engineering, University of Hong Kong, Pokfulam Road, Hong Kong*

A. B. Djurišić<sup>a)</sup>

*Department of Electrical and Electronic Engineering and Department of Physics, The University of Hong Kong, Pokfulam Road, Hong Kong*

W. K. Chan

*Department of Chemistry, The University of Hong Kong, Pokfulam Road, Hong Kong*

J. Gao

*Department of Physics, The University of Hong Kong, Pokfulam Road, Hong Kong*

H. F. Lui and C. Surya

*Department of Electronic and Information Engineering, Hong Kong Polytechnic University, Hung Hom, Kowloon, Hong Kong*

(Received 27 March 2003; accepted 8 May 2003)

The morphology and optical properties of ZnO nanostructures prepared by thermal evaporation of Zn under different conditions was investigated. ZnO nanostructures prepared in air, dry and humid argon flow, and dry and humid nitrogen flow were characterized by scanning electron microscopy, transmission electron microscopy, x-ray diffraction, and photoluminescence. Tetrapod nanorods were obtained for fabrication in air, while for fabrication in argon or nitrogen flow nanowires and tetrapod nanorods were obtained. Growth of nanowires from the end of the tetrapod nanorod was observed. Influence of the preparation conditions on the structure and the room-temperature photoluminescence is discussed. © 2003 American Institute of Physics.  
[DOI: 10.1063/1.1589184]

Semiconductor nanostructures have been attracting increasing attention due to their exceptional properties, which are different from bulk materials. Among these materials, ZnO is of great interest for photonic applications due to its wide band gap (3.37 eV) and large exciton binding energy (60 meV). Different fabrication methods have been reported for ZnO nanoparticles,<sup>1,2</sup> and one-dimensional nanostructures.<sup>3-13</sup> For one-dimensional nanostructures, different shapes (tetrapod nanorods,<sup>6,12</sup> nanowires,<sup>4,5,7-11</sup> or nanobelts<sup>3,13</sup>) were reported. Synthesis of ZnO tetrapod nanorods by oxidation of Zn powder<sup>6</sup> and evaporation of mixture of Zn and silica powder with Fe<sub>2</sub>O<sub>3</sub> used as a catalyst were reported.<sup>12</sup> For ZnO nanowires, fabrication by evaporation of mixture of ZnO and graphite powders,<sup>4,8</sup> Zn powder and Au nanoparticles,<sup>7</sup> ZnO powders,<sup>5</sup> Zn powders,<sup>9,10</sup> and Zn and Se powder<sup>11</sup> were reported. The temperature of evaporation varied from 450 °C (Ref. 9) to 1400 °C.<sup>3</sup> Fabrication in different atmospheres, such as air;<sup>6,8</sup> argon flow;<sup>3,4,9,10</sup> mixture of argon, and oxygen;<sup>7,13</sup> and mixture of argon, oxygen, and hydrogen;<sup>11</sup> were reported. The obtained products were most frequently described as white spongy or fluffy material,<sup>5-9</sup> though gray color,<sup>4,5</sup> yellow,<sup>10</sup> and dark red<sup>11</sup> materials were reported as well.

In this work, the morphology and luminescent properties of ZnO nanostructures prepared under different conditions [in air (no flow), argon and nitrogen flow, with or without

water vapor] were studied to investigate the influence of oxygen availability on the growth of nanostructures and the visible photoluminescence, which is typically attributed to oxygen vacancies.<sup>14</sup> Zn powder was evaporated in a quartz tube at 950 °C. The quartz tube was inserted after the furnace has reached the desired temperature and, for Ar and N<sub>2</sub> flow, gas flow at rate 0.7 l per min was established. For deposition in humid gas flow, the gas was passed through water before being introduced into the furnace. In all cases, white deposition products were obtained except for dry nitrogen flow, which yielded a mixture of white and gray products. The structure of deposited materials was investigated by x-ray diffraction (XRD) using a Siemens D5000 x-ray diffractometer, scanning electron microscopy (SEM) using Cambridge-440 SEM, and transmission electron microscopy (TEM) using Philips Tecnai 20 TEM. The room-temperature photoluminescence was measured using a HeCd laser excitation source (325 nm).

Figure 1 shows the representative SEM images of ZnO nanostructures fabricated under different conditions. In all cases, XRD data showed peaks corresponding to wurtzite ZnO. No diffraction peaks from Zn or other impurities were detected. For deposition in air, tetrapod nanorods were observed. At the higher temperature end of the deposition region, large straight rods were obtained for all five deposition conditions [Fig. 1(a), on the right]. In the case of gas flow, a mixture of tetrapod nanorods and nanowires was obtained [Figs. 1(b) and 1(c)], with nanowires growing from the end

<sup>a)</sup>Electronic mail: dalek@hkusua.hku.hk

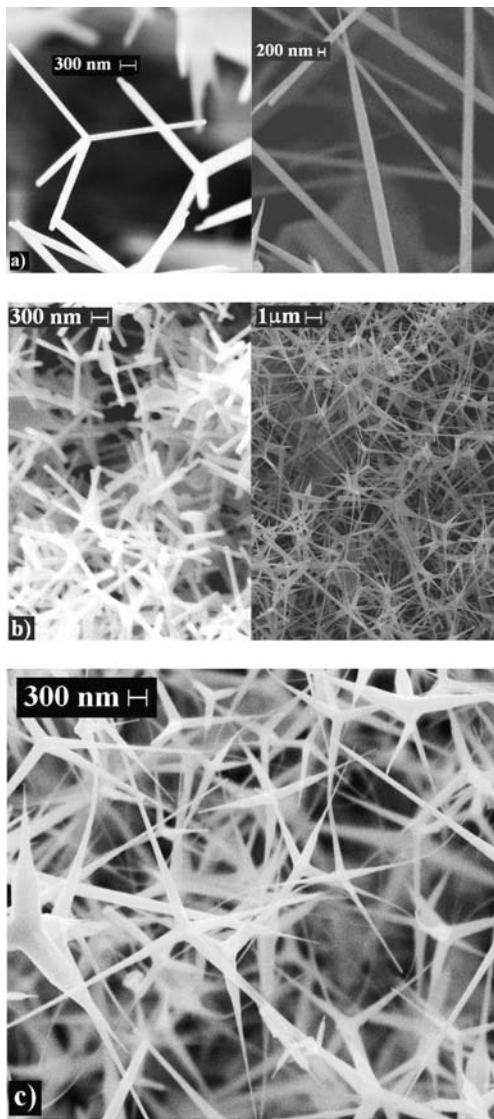


FIG. 1. SEM images of ZnO nanostructures: (a) tetrapods (left) and rods (right) obtained in air; (b) small tetrapods (left) and mixture of tetrapods and wires (right) obtained in dry argon flow; and (c) mixture of tetrapods and wires obtained in humid argon flow.

of tetrapod legs. For the dry argon and dry nitrogen flow, regions with very small tetrapods (submicron length of legs) can also be found. Growth of large tetrapod crystals was demonstrated previously.<sup>15,16</sup> The tetrapod legs of these large tetrapods are single crystal hexagonal ZnO with a [0001] growth direction.<sup>16</sup> Observation of ZnO tetrapod nanorods is similar to the result reported by Dai *et al.*<sup>6</sup> (in air) and Tang *et al.*<sup>12</sup> (in argon flow). There was no report of the nanowires growing out of tetrapod ZnO nanorods. In two previous reports on ZnO tetrapod nanorods<sup>6,12</sup> both vapor–liquid–solid<sup>12</sup> and vapor–solid<sup>9</sup> growth mechanisms were proposed. In our work no catalyst was used, and the obtained results in air were similar to the result reported by Dai *et al.*<sup>6</sup> Therefore, it is likely that the growth mechanism is vapor–solid.

The individual structure of the obtained nanorods and nanowires was studied by TEM. Figure 2(a) shows the TEM images of tetrapod nanorods with beginning stages of nanowire growth from the end of the tetrapod leg. The inset shows an enlarged tetrapod leg–nanowire junction. The junction

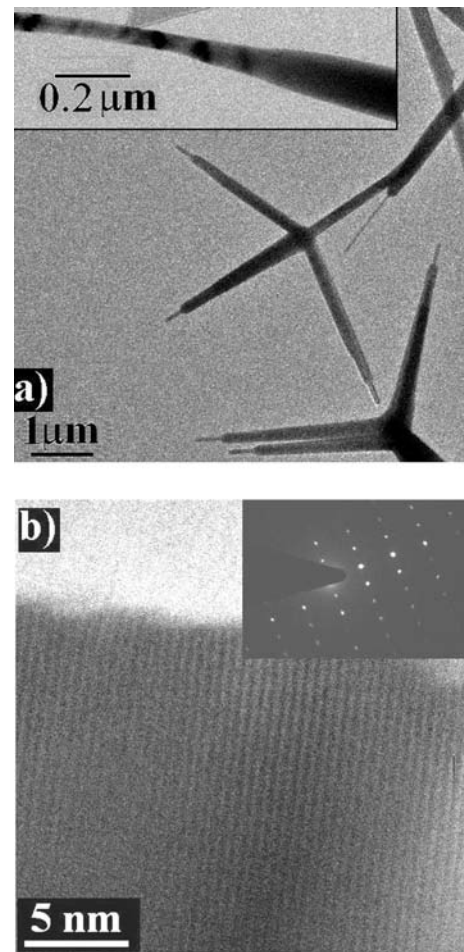


FIG. 2. TEM image of (a) nanowire growing out of a tetrapod leg; inset shows a higher magnification image of the nanowire–tetrapod leg junction. (b) HR TEM of the ZnO nanowire. Inset shows the selected area electron diffraction pattern.

region, typically, shows a ripple-like contrast, which is most likely due to strain. Figure 2(b) shows a high resolution (HR) TEM image, while the inset shows a selected area electron diffraction pattern. Clear lattice fringes, indicating a single crystalline structure, can be observed. In some cases, a very thin amorphous layer can be found on the wires, which is similar to the result reported by Yao *et al.*<sup>8</sup> The spacing between two adjacent lattice planes is about 2.6 Å, indicating growth along the [0001] direction, which is in agreement with two previous reports on the growth direction of ZnO nanowires.<sup>4,8</sup> It is possible that the growth mechanism in this case is similar to that of the growth of GaN nanowires from the sides of hexagonal GaN crystal platelets.<sup>17</sup> It was found that the increase of the NH<sub>3</sub> flow rate suppressed the growth of the nanowires.<sup>17</sup> Thus, the growth of GaN nanowires from the side of the platelets was mainly due to platelet growth being limited by the N atom supply.<sup>17</sup> In our work, oxidation of Zn in inert gas flow likely results in a limited oxygen supply, so that the nanowires grow from the end of the tetrapod legs. Oxidation of Zn in air resulted in the formation of tetrapod nanorods only, with no nanowires found. Further study is needed to determine the structure of the nanowire nucleation sites at the end of the tetrapod legs and the growth kinetics.

Figure 3 shows the room-temperature photolumines-

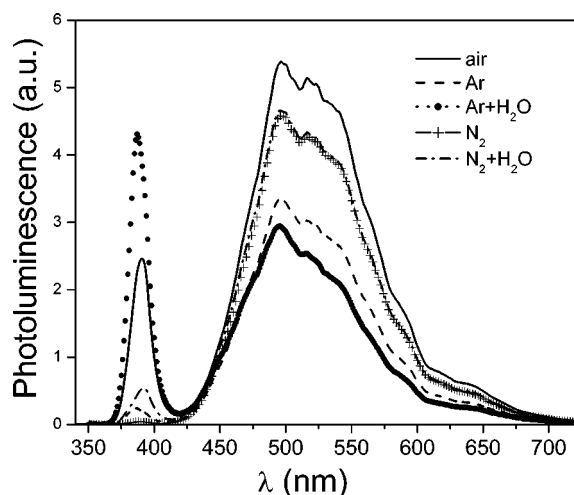


FIG. 3. Photoluminescence of ZnO nanostructures prepared under different conditions.

cence (PL) of ZnO nanostructures prepared under different conditions. In addition to the emission in UV region, broad visible emission can be observed where two main peaks can be identified ( $\sim 495$  and  $\sim 520$  nm), which is similar to the results reported by Park *et al.*<sup>5</sup> A previous study on ZnO tetrapod nanorods also found a broad peak at  $\sim 495$  nm.<sup>6</sup> It can be observed from Fig. 3 that the ratio of the UV to visible emission, as well as the contribution of different observed transitions in the visible spectral range, is clearly dependent on the fabrication conditions. It was reported that the ratio of UV to green emission is dependent on the nanostructure size.<sup>4</sup> However, no clear conclusions on the size versus ratio of UV intensity to green emission can be drawn from our results. The UV emission is stronger than the visible emission for the sample prepared in humid argon flow, which contains smaller nanostructures than the sample prepared in air. Therefore, it is likely that other factors also play a role in the obtained PL result. There is no consensus in the literature on the positions of the peaks in the PL spectrum of ZnO nanostructures and thin films and their origin. The most commonly observed feature is the strong green emission. The work of Vendhausen *et al.*<sup>14</sup> assigned green emission at 510 nm to the transition between the photoexcited holes and singly ionized oxygen vacancy, but this transition has been given as an explanation for the visible emission from 495 nm (Ref. 6) to 583 nm.<sup>18</sup> The green luminescence in ZnO was also attributed to antisite oxygen<sup>19</sup> and donor-acceptor complexes.<sup>20,21</sup> Surface states have also been identified as the possible cause of the visible emission in ZnO nanowires<sup>8</sup> and nanoparticles.<sup>1</sup> It is likely that the visible emission from ZnO cannot be fully explained by a single type of defect. Further study is in progress to identify the origin of the observed peaks and the changes introduced by different gas flows. Nitrogen acts as an acceptor in ZnO (Ref. 22) while calculations indicate that hydrogen can act as a shallow donor,<sup>23</sup>

so that it is difficult to conclusively identify causes of the observed differences in the PL spectrum for different preparation conditions.

To summarize, we have fabricated ZnO nanostructures in air and under argon and nitrogen gas flow (with or without water vapor). A mixture of tetrapod nanorods and nanowires was obtained for the gas flow, while for deposition in air only tetrapod nanorods were observed. The difference in obtained morphologies between deposition in gas flow and atmosphere is likely due to a difference in the availability of oxygen for tetrapod growth. While similar structures were observed for the flow of different gases, the photoluminescence spectrum showed significant differences in the ratio of UV and visible emission. Nanostructures fabricated in humid argon flow showed higher UV than green emission and had smaller average sizes than tetrapod nanostructures obtained in air showing stronger green than UV emission. Therefore, other factors than the nanostructure size can also play a role in the ratio of UV to visible emission in ZnO.

The authors would like to thank Amy Wong and Wing Sang Lee for the SEM and TEM measurements and Dr. M. H. Xie for useful discussions.

- <sup>1</sup>S. Monticone, R. Tufeu, and A. V. Kanaev, *J. Phys. Chem. B* **102**, 2854 (1998).
- <sup>2</sup>S. Mahamuni, K. Borgohain, B. S. Bendre, V. J. Leppert, and S. H. Risbud, *J. Appl. Phys.* **85**, 2861 (1999).
- <sup>3</sup>Z. W. Pan, Z. R. Dai, and Z. L. Wang, *Science* **291**, 1947 (2001).
- <sup>4</sup>M. H. Huang, Y. Wu, H. Feick, N. Tran, E. Weber, and P. Yang, *Adv. Mater. (Weinheim, Ger.)* **13**, 113 (2001).
- <sup>5</sup>K. Park, J. S. Lee, M. Y. Sung, and S. Kim, *Jpn. J. Appl. Phys., Part 1* **41**, 7317 (2002).
- <sup>6</sup>Y. Dai, Y. Zhang, Q. K. Li, and C. W. Nan, *Chem. Phys. Lett.* **358**, 83 (2002).
- <sup>7</sup>Y. W. Wang, L. D. Zhang, G. Z. Wang, X. S. Peng, Z. Q. Chu, and C. H. Liang, *J. Cryst. Growth* **234**, 171 (2002).
- <sup>8</sup>B. D. Yao, Y. F. Chan, and N. Wang, *Appl. Phys. Lett.* **81**, 757 (2002).
- <sup>9</sup>S. C. Lyu, Y. Zhang, H. Ruh, H. J. Lee, H. W. Shim, E. K. Suh, and C. J. Lee, *Chem. Phys. Lett.* **363**, 134 (2002).
- <sup>10</sup>J. Y. Li, X. L. Chen, H. Li, M. He, and Z. Y. Qiao, *J. Cryst. Growth* **233**, 5 (2001).
- <sup>11</sup>Y. C. Kong, D. P. Yu, B. Zhong, W. Fang, and S. Q. Feng, *Appl. Phys. Lett.* **78**, 407 (2001).
- <sup>12</sup>C. C. Tang, S. S. Fan, M. L. de la Chapelle, and P. Li, *Chem. Phys. Lett.* **333**, 12 (2001).
- <sup>13</sup>J. Zhang, W. Yu, and L. Zhang, *Phys. Lett. A* **299**, 276 (2002).
- <sup>14</sup>K. Vanhausden, W. L. Warren, C. H. Seager, D. R. Tallant, J. A. Voigt, and B. E. Gnade, *J. Appl. Phys.* **79**, 7983 (1996).
- <sup>15</sup>H. Iwanaga, M. Fujii, M. Ichihara, and S. Takeuchi, *J. Cryst. Growth* **141**, 234 (1994).
- <sup>16</sup>M. Kitano, T. Hanabe, S. Maeda, and T. Okabe, *J. Cryst. Growth* **108**, 277 (1991).
- <sup>17</sup>M. He, P. Zhou, S. Noor Mohammad, G. L. Harris, J. B. Halpern, R. Jacobs, W. L. Sarney, and L. Salamanca-Riba, *J. Cryst. Growth* **231**, 357 (2001).
- <sup>18</sup>J. W. Hu and Y. Bando, *Appl. Phys. Lett.* **82**, 1401 (2003).
- <sup>19</sup>B. Lin, Z. Fu, and Y. Jia, *Appl. Phys. Lett.* **79**, 943 (2001).
- <sup>20</sup>S. A. Studenikin and M. Cocivera, *J. Appl. Phys.* **91**, 5060 (2002).
- <sup>21</sup>D. C. Reynolds, D. C. Look, and B. Jogai, *J. Appl. Phys.* **89**, 6189 (2001).
- <sup>22</sup>A. B. M. Almamun Ashrafi, I. Suemune, H. Kumano, and S. Tanaka, *Jpn. J. Appl. Phys., Part 2* **41**, L1281 (2002).
- <sup>23</sup>C. G. Van de Walle, *Phys. Rev. Lett.* **85**, 1012 (2000).